scientific reports

Check for updates

OPEN

Ease-of-manufacture highly transparent thin polyvinyl alcohol aerogel

Xiaoli Li[1], Xiao Sun[1], Xuguang Zhang[1], Yi Zheng[1,2]✉ & Marilyn L. Minus[1]

The earliest silicon-based aerogels attracted attention due to their nanoscale porous structure and high transparency. Still, they need to be more balanced with the poor mechanical properties. Their brittle structure limits the development of this promising new material. Therefore, the goal of this work is to optimize the mechanical properties of aerogels while maintaining transparency. The good mechanical properties of polymers have made them the material of choice for this work. Polyvinyl alcohol (PVA), which can undergo self-crosslinking through side-chain hydroxyl groups forming hydrogen bonds, was chosen as the raw material to simplify and expedite the production process. The production process was experimented with, analyzed, and refined. Considering the time efficiency of the experimental process, a one-step gelling method was invented to facilitate the sol-gel transition. The one-step gelling method maintained the high transparency of PVA aerogels and reduced the time required for the gelation process compared to the freeze-thawing method. This work employs carbon dioxide supercritical drying to ensure minimal structural collapse and maximize the porous structure's retention. The transmittance of PVA aerogels can reach up to 93.67% at a wavelength of 1333 nm. The internal structure of aerogels with different PVA concentrations was observed using a Scanning electron microscope. Applying Beer-Lambert's Law eliminated the effect of sample thickness on transparency. The relationship between the transparency of PVA aerogels, their microstructure, and macroscopic concentration was studied and analyzed for the first time. While ensuring light transmittance, the modulus of the PVA aerogel reached as high as 6.18 ± 0.56 MPa at 13 wt%.

The revolutionary material, aerogel, was first introduced by S. S. Kistler in 1932[1]. Aerogels are one material: the skeleton is left by replacing all the liquid with gas in gel without significant collapse. Based on this manufacturing process, aerogels have a unique open porous structure. The gas volume in aerogel can range from 50–99.8%[2]. The ultra-high air volume percentage results in a very low density. First-generation, silicon-based aerogels have high light transmittance and good thermal insulation. However, the application of silicon-based aerogels is hindered by their mechanical properties. Their three-dimensional internal structure is very similar to a pearl necklace, with a 'neck' structure formed by the aging process of silica dissolution and deposition. This part of the connection is relatively weak, and combined with the porous structure of aerogels, it exhibits poor mechanical performance[3]. Polymers are high-molecular-weight materials with unique physical properties, such as toughness and viscoelasticity. This makes polymers a consideration for strengthening silica aerogels or precursors of aerogels. As a result, organic polymer-based aerogels have begun to attract attention. Currently, many organic materials can be made into aerogels, such as resorcinol formaldehyde, phenol formaldehyde, polymethyl methacrylate, and many others[4–6]. Moreover, there are currently some aerogels used for making transparent polymer-based materials. For example, Polyisocyanurate-Polyurethane-Based Aerogels achieve transparency control by varying the concentration of catalysts, with transparency reaching 76% at a wavelength of 532 nm[7]. Polyimide Aerogels have improved transparency through adjustments in the raw material formulation, but polyimides exhibit a yellow tint, making the reduction of this yellow color the next research target for this type of aerogel[8].

Polyvinyl alcohol (PVA) is a colorless and odorless synthetic polymer with water solubility, low toxicity, and biocompatibility. PVA has been used as a precursor for high-modulus, high-strength fibers and highly transparent films[9,10]. The high strength and transparency of PVA products make PVA a consideration for making aerogels. A novel method for preparing silica and PVA hybrid aerogels was invented in 2020. These hybrid silica-PVA aerogels can be used for drug delivery[11]. In the same year, PVA aerogels with a graded microstructure exhibited strong energy storage capabilities and can be used in thermal management components for electronic devices[12]. In 2022, composite aerogels of PVA and silicon retained the excellent mechanical properties of polymers and can

[1]Department of Mechanical and Industrial Engineering, Northeastern University, Boston, MA 02115, USA. [2]Department of Chemical Engineering, Northeastern University, Boston, MA 02115, USA. ✉email: y.zheng@northeastern.edu

be used in industrial applications such as thermal insulation and flame resistance[13]. However, there is limited research focused on the development of the optical properties of PVA aerogels. Therefore, with its outstanding mechanical properties, potential optical performance, and self-crosslinking ability, PVA has been chosen as the raw material for this work.

Aerogels have a unique structure, which leads to many exciting and worth-exploring properties. The aerogel precursor's inherent properties influence these properties but are also affected by the manufacturing process. The impact of different manufacturing processes on the properties of aerogel products cannot be ignored. One classic aerogel preparation process can be divided into three stages[14]. They are the sol formation, sol-gel transition, and gel-aerogel transition processes. The commonly used method in the sol-gel process is the freeze-thawing method. During the freezing time, adjacent cross-linkable parts have enough time to connect, while thawing gives the internal structure more opportunities to form new cross-linked bonds, which are then repeated. The cycles take time, and the cross-linking points formed in different cycles influence the uniformity of the internal structure. The gel-aerogel transition process can also be called the drying process. The drying methods can be classified into three types based on the drying environment: under atmospheric conditions, under freezing, and in a supercritical state. Each method has advantages and disadvantages, and the choice should be made based on the specific research goals.

Many parameters were considered and experimented with to achieve high transparency in PVA aerogels. A supercritical drying method was selected in this work to ensure a better porous structure. After initially determining the production process, PVA aerogels ranging from 2 to 28% have been made. Based on such a wide concentration range, the production process was further refined, and the concentration range that could ensure the production of more stable aerogels was determined. A one-step gelling method for polymer aerogel precursors is researched in this work. This method allows the existence of transparent PVA aerogel and reduces the time required for the gelation process compared to the freeze-thawing method. Additionally, analyzing the fundamental relationship between transmittance and microstructure of aerogels enables this property to become tunable depending on the matrix.

Materials and methods

Materials

This work uses Mowiol 56–98 PVA (Kuraray America Inc) as raw material. The molecular weight of it is about 105,600 g/mol, the degree of hydrolysis is 98.4 ± 0.4 mol%, and the residual acetyl content is 1.5 ± 0.4%. Dimethyl Sulfoxide (DMSO) (CAS # 67-68-5, lot # 472301) was bought from Sigma-Aldrich Corporation. Methanol. The series number of methanol is CAS # 67-56-1, lot # A43420, purchased from Thermo Fisher Scientific. All the materials were used directly without any modification.

Methods

In this work, aerogels are formed through the sol-gel process. The term sol-gel process refers to solid nanoparticles dispersed in a liquid phase, which then aggregate and connect to form a three-dimensional framework that continues to extend within the liquid phase. Regarding the drying process, this work employs carbon dioxide supercritical drying to ensure minimal structural collapse and maximize the porous structure's retention.

Characterization

Scanning electron microscope (SEM)

Scanning electron microscope (SEM) of model Zeiss Surpa 25 was used to observe the internal structure of PVA aerogels. This is a field emission microscope with high resolution. Scanning electron microscopy is a technique that uses a focused electron beam to scan the surface of a sample. The interaction of the electron beam with the atoms on the sample's surface allows for the visualization of the sample's morphology. Therefore, the sample's surface needs to be conductive, meaning that non-conductive polymer samples must be coated with a conductive metal layer. Thus, a Gatan high-resolution ion beam coater was used to apply a 15–20 nm thin layer of gold/palladium on the PVA aerogels. In the sample preparation process, liquid nitrogen is used to immerse the aerogel to make it brittle. Afterward, the aerogel is broken to obtain undamaged cross-sections, allowing for a more accurate observation of the aerogel's pore structure.

Spectrophotometer (V-770)

The transparency of the aerogels was measured using a V-770 UV-visible/NIR spectrophotometer manufactured by JASCO Instrument, with a wavelength range from 190 nm to 2700 nm. This work set the measurement range from 300 to 2500 nm, with a scanning speed of 200 nm/min and a UV/VIS Bandwidth of 5 nm. Using the same testing parameters, transmittance tests were conducted on PVA aerogels ranging from 10 to 15%.

Dynamic mechanical analyzer (DMA)

Tensile tests were conducted using a dynamic mechanical analyzer ($2710-103$ series, manufactured by INSTRON Instrument). Tensile tests were performed on PVA aerogels at different concentrations (ranging from 10 to 15%) that underwent the same formation process. This was done to compare the impact of various concentrations on the mechanical properties of the aerogels.

Results and discussion

Figure 1 shows the sample preparation process, starting with preparing the PVA solution. Next, the solution is dispensed into the molds, followed by the sol-gel process, immersion in the poor solvent for PVA to replace

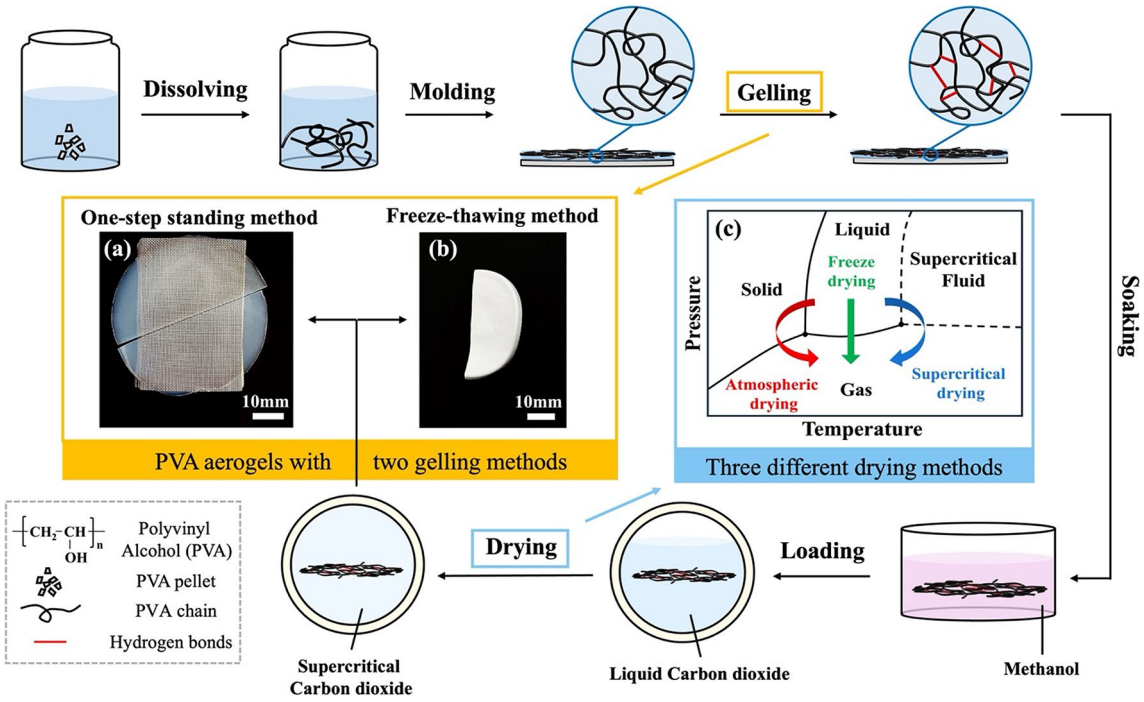

Fig. 1. Schematic diagram showing the new type of aerogel preparation route, and 12% aerogels produced through different gelling methods. (**a**) transparent aerogel produced through the one-step standing method; (**b**) opaque aerogel produced through the freeze-thawing method; (**c**) Phase diagram showing the path of three different drying methods.

DMSO and demolding. Afterward, the wet gel is transferred to a supercritical dryer for carbon dioxide supercritical drying, resulting in PVA aerogels.

Preparation process

Dissolving

Take an appropriate amount of polyvinyl alcohol (PVA) pellets, slowly add them to the DMSO, and then stir. The prepared PVA solution is transparent and viscous. Calculate the volume of DMSO and the corresponding mass of PVA required using Eqs. (1),

$$\frac{x\,[g]}{x\,[g] + 1.1\,\left[\frac{g}{cm^3}\right]\,V\,[ml]} = A\% \tag{1}$$

where x is the mass of PVA; V is the volume of DMSO; $A\%$ is the required concentration percentage of the PVA solution; 1.1 g/cm^3 is the density of DMSO.

Molding

The prepared PVA solution must be transferred to the mold while hot. The choice of mold can control the final shape of the aerogel, which can be films, blocks, columns, and so on. This work focuses on creating thin, uniform, and transparent aerogel sheets. As a result, after a series of mold selections, one type of particular mold was made to achieve this goal.

Sol-Gel process and gelling

The classic sol-gel process was used for this work. Pour the prepared PVA solution onto the preheated molds. With the help of the fluidity of the hot solution itself, the solution spreads thinly and evenly on the mold. The mold is then placed in a sealed container and left to stand in a fume hood at room temperature to allow the long chains of PVA to cross-link and form a three-dimensional network structure. Hydroxyl groups, as side chains of polyvinyl alcohol, can form hydrogen bonds with each other to achieve physical cross-linking. The sample was then soaked in PVA-poor solvent (methanol), which can replace DMSO to obtain a wet gel. They were soaked for three days and replaced every 24 h with a fresh batch of pure methanol to speed up the replacement process.

Physical cross-linking was performed in this work instead of introducing any chemical cross-linking agents. A standard method for physically cross-linking PVA hydrogels is the freeze-thawing method. As the name suggests, the freeze-thawing method involves repeated freezing and thawing cycles. During the freezing process, the crystallized state of the solvent limits the movement of the polymer chains, allowing adjacent hydroxyl groups enough time to form hydrogen bonds for physical cross-linking. Subsequently, the sample is thawed to restore the movement of the polymer chains, allowing more unpaired hydroxyl groups to come closer for a

new round of freezing cross-linking. This repeated freeze-thawing cycle is used to maximize the formation of hydrogen bonds between molecular chains, thereby building a three-dimensional network. Since the freeze-thawing process generally requires three or more cycles, although the time and temperature of each cycle are consistent, it is not easy to ensure that the crosslinking points formed in different cycles are uniform and do not exhibit variations in density. In other words, the cross-linking process performed in different cycles results in significant differences in pore size within the three-dimensional network, limiting pore size uniformity within the aerogel. However, one essential factor related to aerogels' transparency is their internal structure's homogeneity. Therefore, this work attempts a one-step crosslinking method to avoid the occurrence of non-uniform pore sizes due to the presence of solvent crystalline states, giving all hydroxyl groups an equal chance to form hydrogen bonds simultaneously.

The specific operation of the freeze-thawing cycles used in this work is to transfer the prepared solution and the mold to a refrigerator for 24 h (at a temperature of approximately 4 ℃). After freezing, the solution was no longer fluid and was removed and placed in a fume hood to thaw for 12 h (at a temperature of approximately 23 °C). This process is repeated for two cycles, and then a final freezing step is conducted. Finally, the frozen sample is directly immersed in methanol for replacement. In other words, the solution transferred into the mold will undergo a freezing (4 ℃/24 h) - thawing (23 ℃/12 h) - freezing (4 ℃/24 h) - thawing (23 ℃/12 h) - freezing (4 ℃/24 h) - immersion in methanol cycle.

The one-step standing process involves placing the molded solution in a fume hood for 24 h for physical cross-linking and then directly immersing it in methanol. From an experimental procedure perspective, the one-step formation process is more straightforward and time-saving. Regarding the final aerogels, as shown in Fig. 1a, a 12% aerogel was produced through the one-step standing method with high transparency. Figure 1b shows the 12% aerogel produced through the freeze-thawing method has very low transparency.

Soaking

The purpose of the soaking process is to replace DMSO, which can dissolve PVA, with methanol, a poor solvent for PVA, as completely as possible. This aims to retain the three-dimensional network formed by the PVA skeleton only, known as the wet gel. The displacement process is based on the concentration difference of solvent between the inside and outside of the gel. Ideally, when pure methanol is replaced every 24 h, the longer the soaking time, the more complete the replacement, and the residual DMSO should reach 0%. However, in practice, it is impossible to remove DMSO altogether. Still, considering practical limitations and time efficiency during the experiment, the remaining DMSO should be kept as close to 0% as possible. Daily thermal gravimetric analysis (TGA) was conducted on PVA wet gels ranging from 10 to 15% to find the shortest soaking duration. The residual amount of DMSO was recorded daily while replacing an equal amount of methanol. The specific procedure of the thermal analysis was as follows: Ramp 5 ℃/min to 65 ℃, then isothermal at 65 ℃ for 10 min, followed by ramping at 5 ℃/min to 190 ℃ and an isothermal hold at 190 ℃ for 10 min. The selection of these two temperatures is based on the boiling point of methanol at 64.96 ℃ and the boiling point of DMSO at 189 ℃. The two isothermal temperatures were set slightly above the boiling points of methanol and DMSO, respectively. Isothermal for 10 min at each selected temperature allows both solvents to have enough time to evaporate. Then, calculate and compare the residual amount of DMSO for each day to find the plateau. Figure 2 shows that 10–15% of PVA gels reached a plateau in residual DMSO content on the third day. Therefore, in the daily replacement of methanol, the replacement time is set to three days.

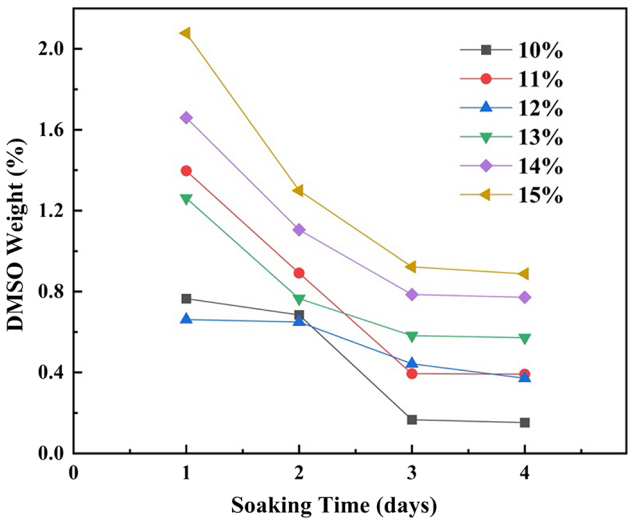

Fig. 2. During the displacement process, the plot of the DMSO residual weight over time for 10–15% PVA wet gels.

Drying

Figure 1c shows the path of three different drying methods in the phase diagram. This work employs carbon dioxide supercritical drying to ensure minimal structural collapse and maximize the porous structure's retention. Carbon dioxide has a critical temperature of 304.13 K (30.98 ℃) and a critical pressure of 73.77 bar (1069.94 psi). The drying process involves transferring the wet gels after displacement (methanol displaces DMSO) to the supercritical dryer. Liquid carbon dioxide is then siphoned into the chamber of the dryer to soak the samples, displacing methanol with liquid carbon dioxide and leaving only liquid carbon dioxide in the gel pores. Every 24 h, all the liquid in the chamber must be released, and new liquid carbon dioxide is siphoned in. Since carbon dioxide can maintain a liquid state only under high pressure, it turns into gas upon release. Therefore, all the liquid released from the chamber is methanol. Completion of displacement can be assessed by observing whether the liquid is still being released from the chamber. Based on this characteristic, it was determined that the displacement process takes two days. On the third day, there was no more liquid coming out. To ensure completeness, a final siphon of new liquid carbon dioxide was done after releasing it on the third day, and then the drying process could be immediately initiated.

An E3100 critical point dryer from Electron Microscopy Sciences company was used in this work. The chamber of the dryer is designed with a double-layer structure. The inner layer is the chamber where the samples are placed. The outer layer has inlets and outlets for circulating hot water to heat the inner chamber. Heating the outer layer with circulating hot water can increase the temperature and pressure in the inner chamber and make the carbon dioxide reach a supercritical state. The dryer is equipped with temperature and pressure gauges and a vent valve to control the internal pressure. Typically, the pressure is regulated at 1200 psi, and the temperature is increased to 35 ℃. The chamber is maintained for 90 min to ensure all carbon dioxide is supercritical. After that, a slow depressurization ensures the carbon dioxide returns to the gaseous state, avoiding the state transition process across the boundary between liquid and gas. This helps prevent structural collapse due to surface tension.

Challenges

During the development process of aerogel formulations, some challenges were encountered. Experiments were conducted on aerogels with concentrations of PVA ranging from 2 to 28%. Initially, the challenge faced was that the finished aerogels were uneven and curled after drying, as shown in Fig. 3a, b, and c. When the concentration was too low (below 10%), the concentration of PVA chains in the solution was insufficient to form a stable three-dimensional network structure. It was unable to maintain a sheet-like morphology when immersed in methanol but dispersed into floccules or small pieces. Figure 3d, e, and f show that increasing the concentration of the aerogel can partially resolve the issue of shape, gradually leading to smoother, sheet-like samples. Then, attempts were made to further address this issue using the freeze-thawing method, as samples in a crystalline state after freezing would avoid immediate dispersion upon immersion in methanol. However, during the high-temperature and high-pressure drying process, the problem of not maintaining a flat sheet-like form still occurred due to the instability of the skeleton structure.

Gradually, the PVA concentration was increased, and minor improvements were made to the experimental process, gradually achieving flat aerogels. To further obtain aerogels with higher transparency, the formulation was further improved. A one-step gelation method was adopted to obtain aerogels with higher transparency. However, new challenges were encountered; when the concentration was too high (above 15%), the viscosity of the solution became too high. This led to the formation of many bubbles during the dissolution and pouring of the solution, resulting in non-uniform bubbles within the sample, significantly affecting the transparency of the aerogel, as shown in Fig. 3g, h, and i. Therefore, it was finally decided to control the PVA concentration within

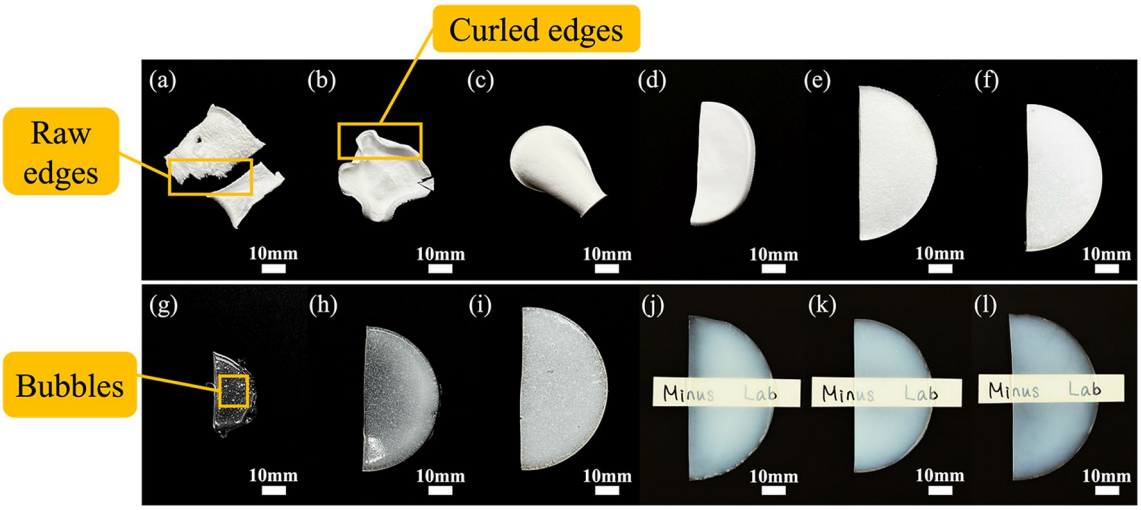

Fig. 3. Opaque Aerogels of different weight percentages: (**a**) 2%; (**b**) 4%; (**c**) 10%; (**d**) 12%; (**e**) 20%; (**f**) 28%; transparent aerogels with bubbles of different weight percentages: (**g**) 20%; (**h**) 24%; (**i**) 28%; transparent and uniform aerogels of different weight percentages: (**j**) 10%; (**k**) 13%; (**l**) 15%.

the safe range of 10–15% to ensure continuous stable production of aerogels with smooth, uniform, and highly transparent morphology, as shown in Fig. 3j, k, and l.

Properties

Mechanical properties

With the increase in PVA concentration in the sample, the number of free hydroxyl groups also increases. Although an increase in hydroxyl groups can facilitate the formation of hydrogen bonds to establish a three-dimensional network structure, there are many factors that influence the formation of this network, including the crystallinity of the sample, the number of hydrogen bonds, and the uniformity of their distribution. Hydroxyl groups are side groups on the long chains of PVA, and their ability to come close enough to form hydrogen bonds is also related to the rigidity of the PVA chains. Therefore, the concentration and mechanical properties cannot be theoretically assumed to have a simple linear relationship. In this work, the effect of concentration on mechanical performance is summarized through experiments. Tensile tests were conducted using a dynamic mechanical analyzer (2710 – 103 series, manufactured by INSTRON Instrument). Tensile tests were performed on PVA aerogels at different concentrations (ranging from 10 to 15%) that underwent the same formation process. This was done to compare the impact of various concentrations on the mechanical properties of the aerogels. From Fig. 4, the sample with a 13% concentration has the highest Young's modulus, reaching 6.18 ± 0.56 MPa. The Young's modulus of regular PVA film is 2.32 ± 0.3 MPa[15]. Based on the data from the graph, it is evident that PVA aerogels, despite having a porous structure, can still maintain the excellent mechanical properties of PVA. In some cases, they even exhibit a higher Young's modulus.

Morphology

SEM tests were conducted on 10–15% of PVA aerogels to compare their internal structures. To easily observe their internal structures, it was necessary to expose the cross-sections of the aerogels. PVA aerogels are very flexible and resilient, making them difficult to break directly. If cut with a knife, the cutting process exerts external pressure on the aerogels, leading to the collapse of the three-dimensional network. Liquid nitrogen (at a temperature of approximately − 195 ℃) was used to make the aerogel brittle, allowing for easy breaking and obtaining relatively intact cross-sections. As mentioned earlier, the sample surface for SEM observation needs to be conductive, so a sputter coater was used to coat the samples. The sputter coater could sputter 2 nm platinum (Pt) grains onto the sample surface in this work. Figure 5 shows SEM images of 10–15% aerogels at different magnifications. When observed horizontally in the images, it is easy to compare the internal structure morphology at the same concentration but different magnifications. When observed vertically, it allows for comparing the internal structures of aerogels at the same magnification but at different concentrations. Vertical observation in Fig. 5 shows that the internal pore distribution of 10% and 11% PVA aerogels is relatively uniform. Starting from 12%, it is observed that some PVA chains begin to crowd together, and this crowding continues until the 14% PVA aerogel, where crowded PVA clusters are still present. The proximity of polymer chains results in a gradation of pore sizes. This means that the pores between PVA clusters are more prominent, approximately in the range of a few hundred nanometers. When the magnification is further increased, numerous secondary pores are found within each large pore, and their sizes are on the same order of magnitude as the pores in the 10% and 11% PVA aerogels. Further observing of the SEM image of the 15% PVA aerogel reveals that the pore gradation has been mitigated, and the distribution of PVA chains appears more uniform.

Panels (a) to (f) represent PVA aerogels of different concentrations from 10 to 15%, while subpanels (1) to (3) represent magnifications of 5000x, 30,000x, and 60,000x, respectively.

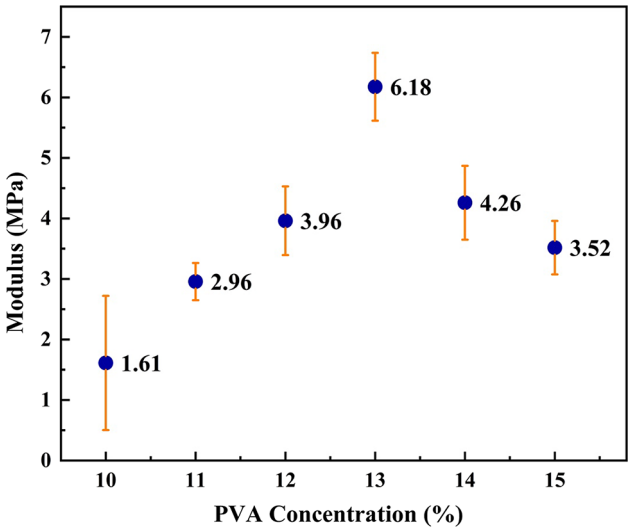

Fig. 4. Tensile modulus for PVA Aerogels with different concentrations.

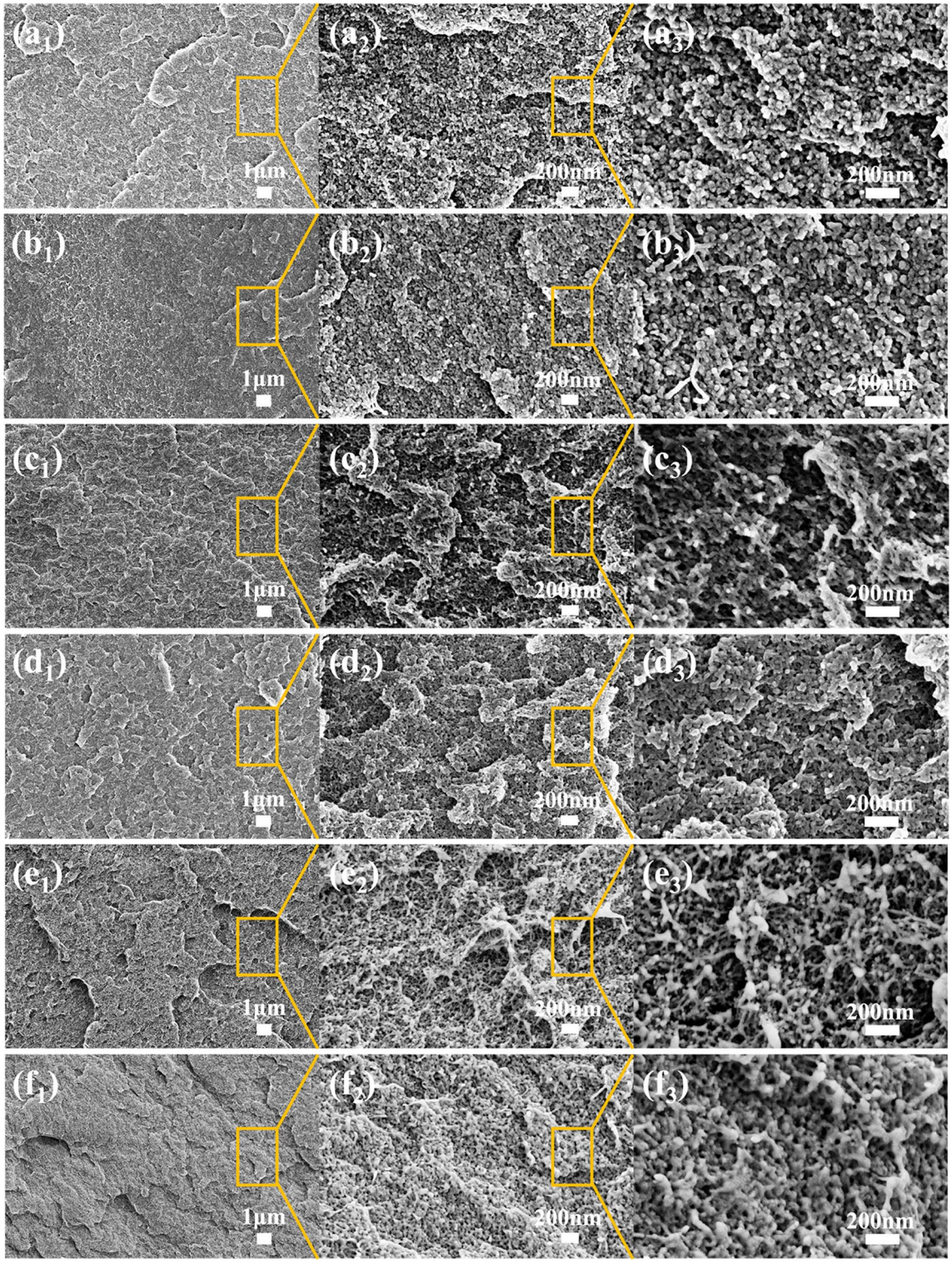

Fig. 5. SEM images of PVA aerogels at different magnifications and concentrations.

The pore size and particle size data were obtained by analyzing SEM images using ImageJ, with each data point based on an average of 50 measurements. The standard deviation was also recorded. The size of the standard deviation corresponds to the uniformity of the pores. From Fig. 6, the samples are ranked from lowest to highest standard deviation as follows: 10%, 11%, 15%, 14%, 13%, and 12%. This means that the 10% sample has the best pore uniformity, while the 12% sample has the worst. Similarly, for PVA aerogels with concentrations ranging from 10 to 15%, their pore sizes are of the same order of magnitude. Regarding light scattering, there are two classical definitions: Rayleigh Scattering and Mie Scattering. Rayleigh Scattering refers to the scattering that

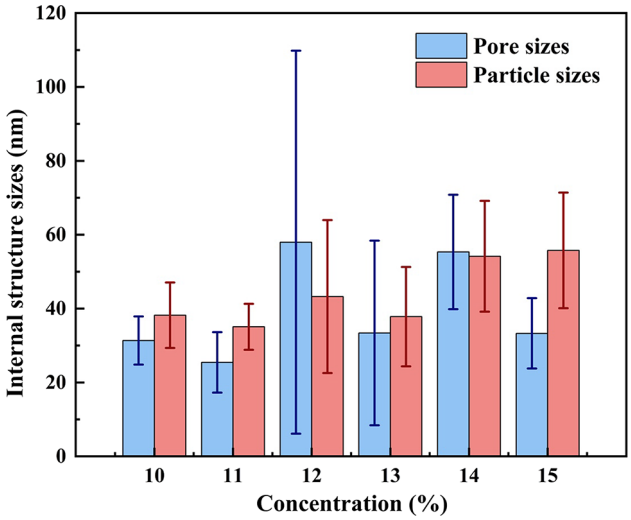

Fig. 6. Pore sizes and particle sizes of PVA aerogels with different concentrations ranging from 10 to 15%.

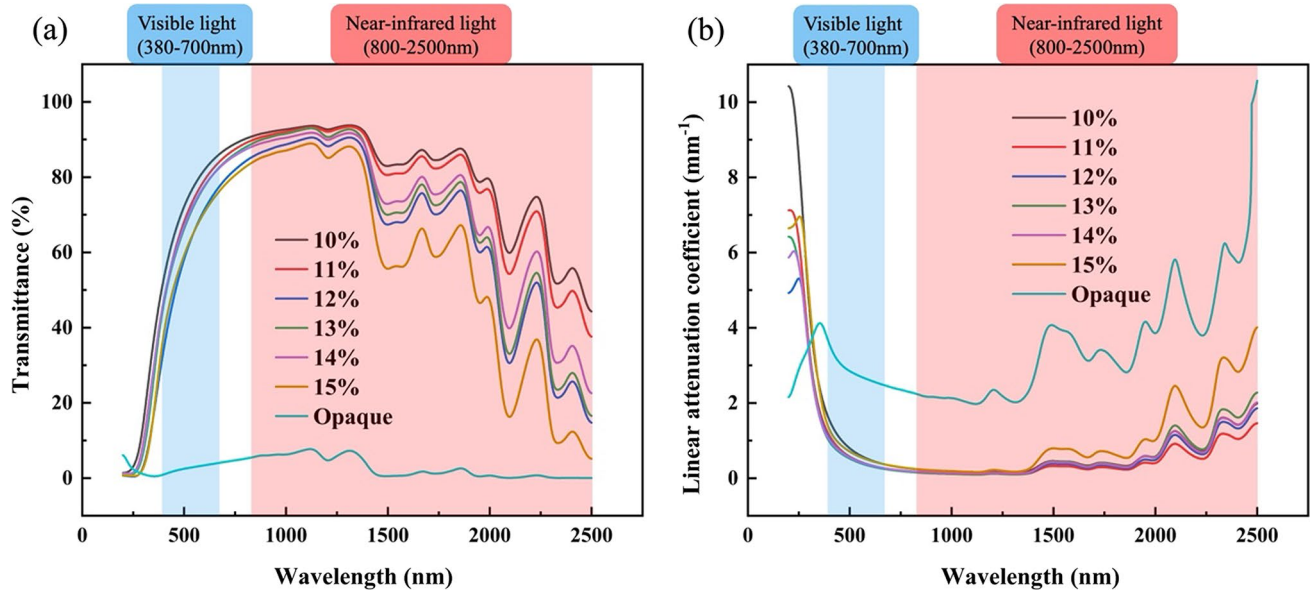

Fig. 7. (**a**) The transmittance curves for transparent PVA aerogels ranging from 10–15% and opaque PVA aerogel; (**b**) The curves of linear attenuation coefficient versus the wavelength for PVA aerogels ranging from 10–15% and opaque PVA aerogel.

occurs when the particle size is much smaller than the wavelength, typically explaining everyday phenomena such as why the sky is blue and why it turns red at sunset. Mie Scattering, on the other hand, refers to scattering when the particle size is equal to or larger than the wavelength, which often explains the phenomenon of brownish smog. By considering the skeleton width in SEM images of PVA aerogels as the particle diameter, and performing at least 50 measurements, we can determine the particle size within the internal structure of samples with concentrations from 10 to 15%. The particle sizes within PVA aerogels at different concentrations are quite different compared to the wavelength, leading to Rayleigh Scattering when light interacts with the material. This also explains why PVA aerogels exhibit a light blue color.

Transmittance

Transmittance tests were conducted on PVA aerogels ranging from 10 to 15%. The tests were performed using a V-770 UV-Visible/NIR spectrophotometer with a measurement range set from 300 to 2500 nm, a scanning speed of 200 nm/min, and a UV/VIS bandwidth of 5 nm. Figure 7a shows the curves comparing transmittance with wavelength for PVA aerogels of different concentrations. The 10% sample exhibited higher transmittance. The wavelength range within the blue box in Fig. 7 represents the visible light range, while the red box indicates the near-infrared light range. At a wavelength of 1333 nm, the transmittance reaches its highest value of 93.67%.

Transmittance is influenced not only by the sample's internal structure but also by the thickness. Since the directly tested samples had slightly varying thicknesses, this work accounted for the thickness effect on transmittance using Beer-Lambert's law[16],

$$T = e^{-\alpha x} \tag{2}$$

where T is transmittance [%]; x is the thickness of aerogel [mm]; α is linear attenuation coefficient [mm^{-1}]. The linear attenuation coefficient refers to the difficulty of propagation of specific physical quantities, such as photons, sound waves, and electrons, in a material along a single direction. For assessing the transparency of materials, a higher linear attenuation coefficient of the material itself implies that light entering the material will rapidly attenuate. In contrast, a lower linear attenuation coefficient suggests light can more easily pass through the material. In other words, the linear attenuation coefficient for different concentrations of PVA aerogel is calculated by eliminating the effect of the PVA aerogel's thickness. A lower coefficient represents a more transparent material.

From Fig. 7b, it can be observed that the aerogels prepared by the one-step standing method exhibit excellent light-transmitting ability, regardless of concentration, which is far superior to the opaque aerogels produced by the freeze-thawing method. In the 700 nm to 1300 nm range, the effect of PVA concentration on the aerogel can be ignored, as all one-step standing aerogels exhibit excellent light-transmitting ability. As the wavelength continues to increase, it can be observed that the 11% sample has better light-transmitting ability, while the 15% sample has poorer light-transmitting ability. This can provide some guidance for the application of such aerogels in different fields, helping to balance cost, transparency, and even mechanical and thermal insulation properties to choose the most suitable formulation.

Conclusions

At first, considering the brittleness and poor mechanical properties of the earliest discovered silica aerogels, this drawback limits the application development of aerogels. Therefore, improving the mechanical properties of aerogels was set as the primary goal. Thus, the material selection focused on polymers. The experimental direction was set as pure physical cross-linking without using any cross-linking agents to simplify and expedite the production process. Thus, polyvinyl alcohol (PVA), which can undergo self-crosslinking through side-chain hydroxyl groups forming hydrogen bonds, was chosen as the raw material to attempt aerogel production. Mechanical tests were conducted on transparent PVA aerogels with concentrations ranging from 10 to 15%. The sample with a 13% concentration achieved the highest modulus, reaching 6.18 ± 0.56 MPa.

After the material selection, the production method was experimented with, analyzed, and refined. Comparative analysis of freeze-thawing methods revealed that this approach could not guarantee the transparency of PVA aerogels. Considering the time efficiency of the experimental process, a one-step standing method was invented to facilitate the sol-gel transition. The one-step standing method not only maintained high transparency of PVA aerogels but also reduced the time required for the gelation process compared to the freeze-thawing method. Subsequently, PVA concentrations ranging from 2 to 28% were tested, revealing various challenges, including curling, raw edges at low concentrations, and bubble formation at high concentrations. The production process was further refined, and a safe concentration window of 10–15% was determined, ensuring the production of stable, thin, and transparent PVA aerogel.

Using ImageJ, SEM images of samples with concentrations ranging from 10 to 15% were analyzed, with no fewer than 50 measurements taken for each sample to determine pore sizes. The standard deviation of pore sizes was recorded, as it can represent the uniformity of pore sizes. Pore sizes are within the same order of magnitude for samples with 10% and 15% concentrations, mostly in the tens of nanometers. Additionally, the internal skeleton diameter can be considered the particle size for open-pore structured aerogels. In this work, the particle size of PVA aerogels is much smaller than the wavelength, satisfying the conditions for Rayleigh Scattering, which explains why the aerogels appear light blue. The light transmittance curve and linear attenuation coefficient versus the wavelength curve of the opaque samples were also compared with those of the transparent samples. The opaque samples prepared by the freeze-thawing method have significantly lower transparency than those prepared using the improved one-step standing method developed in this work.

Data availability

The data presented in this study are available on request from the corresponding author.

Received: 7 September 2024; Accepted: 21 October 2024
Published online: 01 November 2024

References

1. Kistler, S. S. Coherent expanded-aerogels. *J. Phys. Chem.* **36**(1), 52–64 (2002).
2. Jo, M.-G., Kim, N.-G. & Kim, H.-J. Fabrication of Sn (IV) porphyrin- imbedded silica aerogel composite. *J. Compos. Sci.* **7**(9), 401 (2023).
3. Salimian, S., Zadhoush, A., Naeimirad, M., Kotek, R. & Ramakrishna, S. A review on aero- gel: 3D nanoporous structured fillers in polymer-based nanocomposites. *Polym. Compos.* **39**(10), 3383–3408 (2018).
4. Schwan, M. & Ratke, L. Flexibilisation of resorcinol–formaldehyde aerogels. *J. Mater. Chem. A* **1**(43), 13462–13468 (2013).
5. Grishechko, L. I. et al. Lignin–phenol–formaldehyde aerogels and cryogels. *Microporous Mesoporous Mater.* **168**, 19–29 (2013).
6. Li, H. et al. Loads transfer across static electrical phase interfaces in silica aerogel/polymethyl methacrylate composites. *Compos. Sci. Technol.* **138**, 169–178 (2017).
7. Merillas, B. et al. Transparent polyisocyanurate-polyurethane-based aerogels: Key aspects on the synthesis and their porous structures. *ACS Appl. Polym. Mater.* **3**(9), 4607–4615 (2021).

8. Vivod, S. L. et al. Toward improved optical transparency of polyimide aerogels. *ACS Appl. Mater. Interfaces* **12**(7), 8622–8633 (2020).
9. Pajonk, G. M. Transparent silica aerogels. *J. Non-Cryst. Solids* **225**, 307–314 (1998).
10. Russo, R. E. & Hunt, A. J. Comparison of ethyl versus methyl sol-gels for silica aerogels using polar nephelometry. *J. Non-Cryst. Solids* **86**(1–2), 219–230 (1986).
11. Leventis, N., Sotiriou-Leventis, C., Zhang, G. & Rawashdeh, A.-M.M. Nanoengineering strong silica aerogels. *Nano Lett.* **2**(9), 957–960 (2002).
12. Pekala, R. W. Low density, resorcinol-formaldehyde aerogels, 10 1989.
13. Smith, D. M., Stein, D., Anderson, J. M. & Ackerman, W. Preparation of low-density xerogels at ambient pressure. *J. Non-Cryst. Solids* **186**, 104–112 (1995).
14. Schultz, J. M., Jensen, K. I. & Kristiansen, F. H. Super insulating aerogel glazing. *Sol. Energy Mater. Sol. Cells* **89**(2–3), 275–285 (2005).
15. Jain, N., Singh, V. K. & Chauhan, S. A review on mechanical and water absorption properties of polyvinyl alcohol based composites/films. *J. Mech. Behav. Mater.* **26**(5–6), 213–222 (2017).
16. Mohanan, J. L. & Brock, S. L. A new addition to the aerogel community: Un- supported CdS aerogels with tunable optical properties. *J. Non-Cryst. Solids* **350**, 1–8 (2004).

Acknowledgements

We would like to thank Professor Ming Su from the Department of Chemical Engineering at Northeastern University and his student, Yutian Yang, for their assistance with BET testing during the review process.

Author contributions

Conceptualization, X.L., Y.Z. and M.L.M.; methodology, X.L.; formal analysis, X.L.; investigation, X.L.; resources, M.L.M.; data curation, X.L. and X.Z.; writing—original draft preparation, X.L.; writing—review and editing, X.L., X.S., Y.Z. and M.L.M.; supervision, Y.Z. and M.L.M.; project administration, Y.Z. and M.L.M.; funding acquisition, Y.Z. and M.L.M. All authors have read and agreed to the published version of the manuscript.

Funding

The authors would like to acknowledge the funding support for this work from Rogers Corporation (Grant number: G00007031) and the National Science Foundation (Grant number: CBET-1941743).

Declarations

Competing interests

The authors declare no competing interests.

Additional information

Correspondence and requests for materials should be addressed to Y.Z.